

Fate of Cd during Microbial Fe(III) Mineral Reduction by a Novel and Cd-Tolerant *Geobacter* Species

E. Marie Muehe,[†] Martin Obst,[‡] Adam Hitchcock,[§] Tolek Tyliszczak,^{||} Sebastian Behrens,[†] Christian Schröder,^{†,▽} James M. Byrne,[†] F. Marc Michel,[⊥] Ute Krämer,[#] and Andreas Kappler^{*,†}

[†]Geomicrobiology, Center for Applied Geosciences, University of Tuebingen, 72076 Tuebingen, Germany

[‡]Environmental Analytical Microscopy, Center for Applied Geosciences, University of Tuebingen, 72074 Tuebingen, Germany

[§]Department of Chemistry and Chemical Biology, McMaster University Hamilton, Hamilton Ontario, Canada L8S 4M1

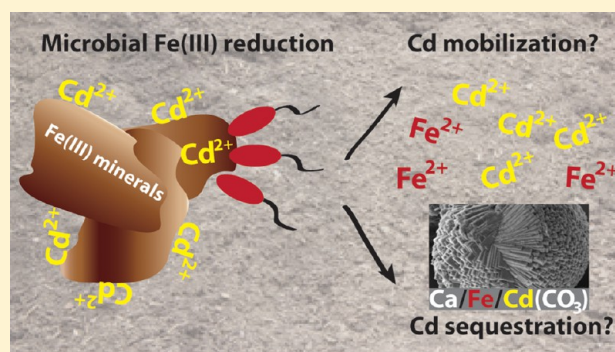
^{||}Advanced Light Source, Lawrence Berkeley National Laboratory, Berkeley, California 94720, United States

[⊥]Department of Geosciences, Virginia Tech, Blacksburg, Virginia 24061, United States

[#]Department of Plant Physiology, Ruhr University Bochum, 44801 Bochum, Germany

S Supporting Information

ABSTRACT: Fe(III) (oxyhydr)oxides affect the mobility of contaminants in the environment by providing reactive surfaces for sorption. This includes the toxic metal cadmium (Cd), which prevails in agricultural soils and is taken up by crops. Fe(III)-reducing bacteria can mobilize such contaminants by Fe(III) mineral dissolution or immobilize them by sorption to or coprecipitation with secondary Fe minerals. To date, not much is known about the fate of Fe(III) mineral-associated Cd during microbial Fe(III) reduction. Here, we describe the isolation of a new *Geobacter* sp. strain Cd1 from a Cd-contaminated field site, where the strain accounts for 10^4 cells g^{-1} dry soil. Strain Cd1 reduces the poorly crystalline Fe(III) oxyhydroxide ferrihydrite in the presence of at least up to 112 mg Cd L^{-1} . During initial microbial reduction of Cd-loaded ferrihydrite, sorbed Cd was mobilized. However, during continuous microbial Fe(III) reduction, Cd was immobilized by sorption to and/or coprecipitation within newly formed secondary minerals that contained Ca, Fe, and carbonate, implying the formation of an otavite-siderite-calcite ($\text{CdCO}_3\text{--FeCO}_3\text{--CaCO}_3$) mixed mineral phase. Our data shows that microbially mediated turnover of Fe minerals affects the mobility of Cd in soils, potentially altering the dynamics of Cd uptake into food or phyto-remediating plants.



INTRODUCTION

The heavy metal cadmium (Cd) is one of the most widely distributed contaminants in agricultural soils worldwide^{1–3} and poses a great threat to environmental and human health.¹ This has been recognized by governmental agencies, which have consequently released new regulations to minimize Cd input into the environment and Cd uptake by humans.⁴ Cd enters the human body via crops and tobacco smoke,¹ and mainly affects kidneys, liver, bones and increases the risk of cancer.^{1,5,6} The input of Cd into agricultural soils occurs via atmospheric deposition and fertilization.^{7–9} Cd binds to clays, carbonates, organic matter, and Fe oxides in soils, with most of the Cd prevailing in the exchangeable fraction, thus becoming easily bioavailable to plants and soil microbiota.^{1,10} So far, research focused on geochemical factors that increase or decrease Cd bioavailability, however, changes in soil mineralogy caused by microorganisms have not yet been thoroughly considered.

Cd was shown to positively correlate with total Fe oxide content in different soils.^{11,12} At circumneutral pH, Cd binds directly to hydroxyl surface groups of Fe and Mn (oxyhydr)-

oxides¹³ or indirectly via ternary complexes with organic matter.¹⁴ Several studies have investigated sorption mechanisms and the impact of competing ions on Cd sorption to various Fe(III) (oxyhydr)oxides.^{15–18} However, Fe is redox active and has a high turnover rate in soils and water.¹⁹ Abiotic and microbial Fe(II) oxidation lead to Fe(III) mineral formation in anoxic and oxic pH-neutral environments.²⁰ The reverse reaction, that is the reduction of Fe(III) to Fe(II), is mainly mediated by Fe(III)-reducing bacteria, which oxidize organic or inorganic electron donors and reduce Fe(III) (oxyhydr)oxides.²¹ During this process, the Fe(III) minerals are partially or completely dissolved and aqueous Fe^{2+} and secondary Fe(II) or Fe(II)/Fe(III) mixed valence mineral phases form depending on the geochemical conditions.²⁰ The formation and dissolution of Fe(III) minerals significantly affect the mobility

Received: July 29, 2013

Revised: November 15, 2013

Accepted: November 25, 2013

Published: November 25, 2013

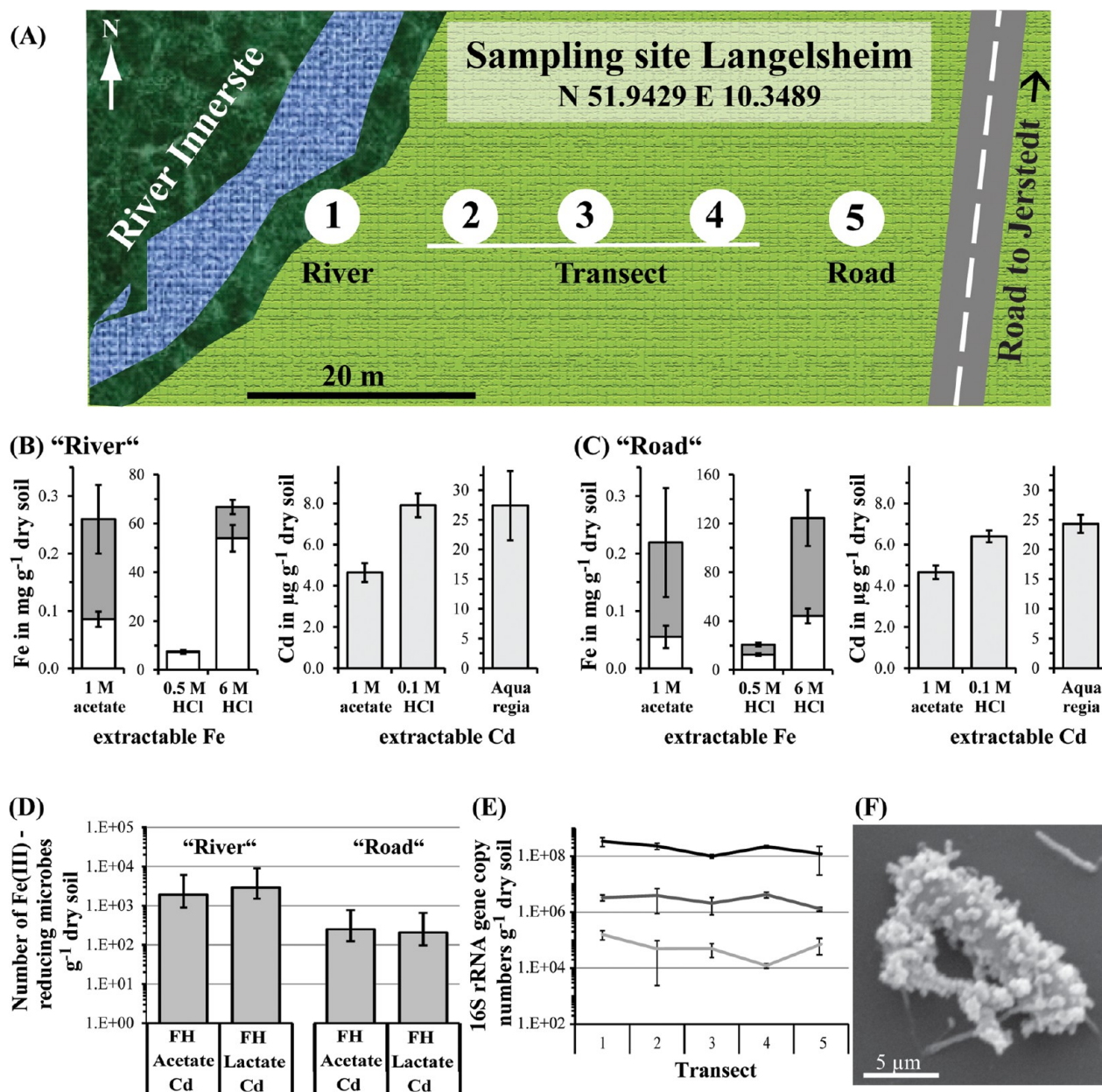


Figure 1. Field site Langelshiem, Goslar, Germany (N51.9429 E10.3489) was sampled in a transect at five different sampling points 1–5 (A). Sampling point 1 is referred to as “river” and sampling point 5 as “road”. The amount of 1 M acetate- and 0.5 and 6 M HCl-extractable Fe (in mg Fe g⁻¹ dry soil, n = 3) are given for “river” (B) and “road” (C). Fe(II) and Fe(III) are depicted in gray and white, respectively. 1 M acetate-, 0.1 M HCl- and aqua regia-extractable Cd (in μg Cd g⁻¹ dry soil, n = 3) is shown for “river” (B) and “road” (C). The presence of bacteria capable of Fe(III) reduction using either acetate or lactate as electron donor is shown for “river” and “road” (D) (in microbes g⁻¹ dry soil, n = 7). 16S rRNA gene copy numbers of total Bacteria (black line), *Geobacter* spp. (dark gray line) and the isolate *Geobacter* sp. Cd1 (light gray line) present in the soil are given for sampling locations 1–5 (E), based on 16S rRNA quantification by qPCR (in 16S rRNA gene copy numbers g⁻¹ dry soil, n = 4). Scanning electron micrograph of strain Cd1 after reduction of Cd-loaded ferrihydrite (F). Mean values ± standard deviation.

and bioavailability of mineral-associated nutrients and contaminants.^{22–24} Up to now, microbial Fe(III) reduction-induced changes of metal(loid) mobility and bioavailability have been studied for a number of metal(loid)s including arsenic,²⁵ radium,²⁶ chromium,^{27,28} and uranium,^{29,30} but not comprehensively for Cd.

The most prominent case of how microbial Fe(III) reduction affects metal mobility currently is observed in Southeast Asia. In that case, Fe mineral-associated As was mobilized by the activity of microorganisms,³¹ which caused the “world’s worst mass poisoning” by contaminating the drinking water of millions of

people.³² During microbially catalyzed reductive dissolution of As-loaded Fe(III) minerals, As can be either mobilized from the minerals or sequestered by newly formed secondary Fe minerals.^{31,33} Fe(III)-reducing microbial communities including the genus *Geobacter* were correlated with the mobilization of As in these aquifers.^{25,34,35} The species *Geobacter metallireducens* is most commonly known for Fe(III) reduction but also for the bioremediation of metal-contaminated soils, including uranium, chromate, and cobalt, but not Cd.^{36–38} To our knowledge, no Fe(III)-reducing bacterium has been isolated that shows high tolerance to Cd. Whether microbial reduction of Cd-loaded

Fe(III) minerals leads to mobilization or sequestration of Cd in secondary Fe mineral phases has not been studied in detail yet.

Within this study, we first isolated a Fe(III)-reducing *Geobacter* strain that shows high Cd tolerance and reduces Fe(III) minerals in the presence of elevated Cd concentrations. In a second step, the ability to reduce Cd-loaded ferrihydrite was determined for the isolated strain in comparison to the known metal-remediator *Geobacter metallireducens* strain GS-15. Finally, Cd mobility, its distribution between the liquid and solid-phase, and the Fe mineralogy were determined during and after microbial reduction of Cd-loaded ferrihydrite.

MATERIAL AND METHODS

Geochemical and Microbiological Field Site Characterization. The Cd-contaminated field site Langelsheim is located adjacent to the Innerste river near Goslar, Germany (N51.9429 E10.3489) (Figure 1a). Five sampling points were selected along a transect between river and road. At sampling points 1 (“river”) and 5 (“road”), the water content, soil pH, total organic and inorganic carbon (TOC and TIC), 1 M Na-acetate-, 0.5 and 6 M HCl-extractable Fe were determined after sieving the soil (2 mm) (see Rijal, et al.³⁹). To determine mobile or loosely sorbed Cd, 1 g of soil was extracted with 10 mL of 1 M ammonium acetate (24 h, 25 °C, 150 rpm). Cd associated with poorly crystalline minerals was extracted from 1 g of soil with 10 mL of 0.1 M HCl (30 min, 25 °C, 150 rpm). After extraction, the soil suspensions were filtered through Whatman No. 1 filter paper and stabilized by 1 mL 65% HNO₃. For aqua regia extractions, 0.25 g soil were extracted with 1.8 mL of 37% HCl and 0.6 mL of 65% HNO₃ for 2 h at 60 °C, 2 h at 75 °C, and 5 h at 100 °C. After cooling to 25 °C, the solution was filled up to 10 mL with 2% HNO₃ and filtered through Whatman No. 1 paper. At sampling points “river” and “road”, the presence of Fe(III)-reducing bacteria with acetate or lactate as electron donor and in the presence of 11 mg L⁻¹ Cd was determined by most probable number (MPN) studies.⁴⁰ 16S rRNA gene copy numbers of total bacteria, Fe(III)-reducing *Geobacter* spp. and the isolated *Geobacter* sp. strain Cd1 were quantified by qPCR. For this, soil samples were frozen at -20 °C.

Isolation and Characterization of a Cd-Tolerant Fe(III)-Reducing Strain. From a Fe(III)-reducer MPN plate of the sampling point ‘river’, 10% (v/v) of an enrichment were transferred to 15 mL volume culture tubes containing 9 mL of anoxic mineral medium⁴¹ and 1.07 g L⁻¹ ferrihydrite (10 mM), 20 mM acetate and 11 mg L⁻¹ total Cd (100 μM). The enrichment was transferred 10 times into fresh medium. The transfers 7–10 included a 10-fold dilution series, from which the highest dilution that showed growth after transfer was used for the following transfer. The purity of the obtained culture was verified microscopically and via 16S rRNA gene cloning and sequencing. After obtaining the isolate *Geobacter* sp. Cd1, the strain was routinely cultivated in the presence of 100 μM Cd at 28 °C. To determine its Cd tolerance, strain Cd1 was incubated with ferrihydrite, acetate and up to 112 mg L⁻¹ (1000 μM) Cd (CdCl₂) and Fe(III) reduction was followed over time. To determine the versatility of Cd1, different electron donors (organic acids, glucose, H₂, Fe(II)) and acceptors (Fe(III), fumarate, nitrate) were tested. Fe redox transformation was quantified with the ferrozine assay,⁴² while growth in the absence of Fe was determined by OD measurements (660 nm).

Competitive Fe(III) Reduction Experiments. *Geobacter metallireducens* strain GS-15⁴³ and *Geobacter* sp. Cd1 were adapted to the experimental growth conditions by growing two consecutive precultures on medium containing 1.07 g L⁻¹ ferrihydrite (10 mM) and 20 mM Na-acetate for 7 days without Cd. For experiments, 50 mL medium were amended with 0.54 or 0.86 g L⁻¹ ferrihydrite (5 or 8 mM), synthesized by neutralization of a Fe^{III}(NO₃)₃ solution using 1 M KOH.¹⁹ 0, 11, or 55 mg L⁻¹ Cd and 20 mM Na-acetate were added prior to inoculation with 5% v/v preculture containing 1.35 × 10⁷ strain Cd1 cells mL⁻¹ or 8.59 × 10⁷ strain GS-15 cells mL⁻¹. During Fe(III) reduction, the pH rose from 7.0 to 7.4 in all set-ups. For analyses, bottles were shaken and 2-mL samples were withdrawn in an anoxic chamber (N₂). For cell number quantification with qPCR, 1-mL samples were frozen at -20 °C. For total Fe analysis, 100 μL sample was added to 0.9 mL of 1 M anoxic HCl, incubated anoxically for 24 h at 4 °C to dissolve minerals and prevent Fe(II) oxidation until quantification.⁴⁴ The remaining 0.9 mL sample was centrifuged (13200g, 2 min). For dissolved Fe, 100 μL supernatant was added to 0.4 mL of 1 M anoxic HCl. For quantification of dissolved Cd, 500 μL supernatant was added to 9.5 mL of 2% HNO₃ and stored at 4 °C until measurement. At the beginning of the experiment, the total Cd content was determined by dissolving 0.25 mL sample in 0.25 mL of 1 M HCl and 9.5 mL of 2% HNO₃. For solid phase analysis, bottles containing 0.86 g L⁻¹ ferrihydrite (8 mM) and 55 mg L⁻¹ Cd were set up for Fe(III) reduction by strain Cd1. Fe–Cd-minerals were harvested by centrifugation, washed three times with anoxic Milli-Q water, and vacuum-dried for Mössbauer, SEM-EDX, and XRD-PDF analysis.

Molecular Biology Methods. DNA from soil and from the isolated strain was extracted, amplified and sequenced as described in the Supporting Information (SI). Details on the quantification of total Bacteria, *Geobacter* spp. and *Geobacter* sp. Cd1 16S rRNA gene copy numbers by qPCR are provided in the SI.

Analytical Methods. Details regarding analysis of Fe and Cd, mineral analysis by Mössbauer spectroscopy, SEM-EDX, synchrotron-XRD, synchrotron total scattering and PDF analysis, and STXM are provided in the SI.

RESULTS

Geochemical and Microbiological Description of the Cd-Contaminated Field Site Langelsheim. The soil pH at the field site Langelsheim was 6.2 ± 0.0, the organic carbon content was between 4.5 and 8% (w/w), and the inorganic carbon was between 0.20 and 1.04% (w/w). The concentrations of sorbed (Na-acetate-extractable) Fe were below 0.3 mg Fe g⁻¹ dry soil at both sampling points “river” and “road” (Figure 1b,c). Poorly crystalline (0.5-M-extractable) Fe was twice as high at “road” than at “river” (approximately 20 vs 10 mg Fe g⁻¹ dry soil) and consisted mainly of Fe(III) at “river” and approximately 50% Fe(II) at “road”. Most Fe was present in the crystalline Fe fraction: Sampling point “road” contained twice as much crystalline Fe (approximately 122 mg g⁻¹ dry soil), made up of 60% Fe(II), compared to sampling point “river” (approximately 65 mg g⁻¹ soil) with 20% Fe(II). Approximately 25 μg total Cd g⁻¹ dry soil were extractable with aqua regia at “road” and “river” (Figure 1b,c). Ammonium acetate extraction revealed approximately 4.5 μg Cd g⁻¹ dry soil in the exchangeable Cd fraction at both sampling points. Approximately 8 and 6 μg Cd g⁻¹ soil were present in the 0.1 M

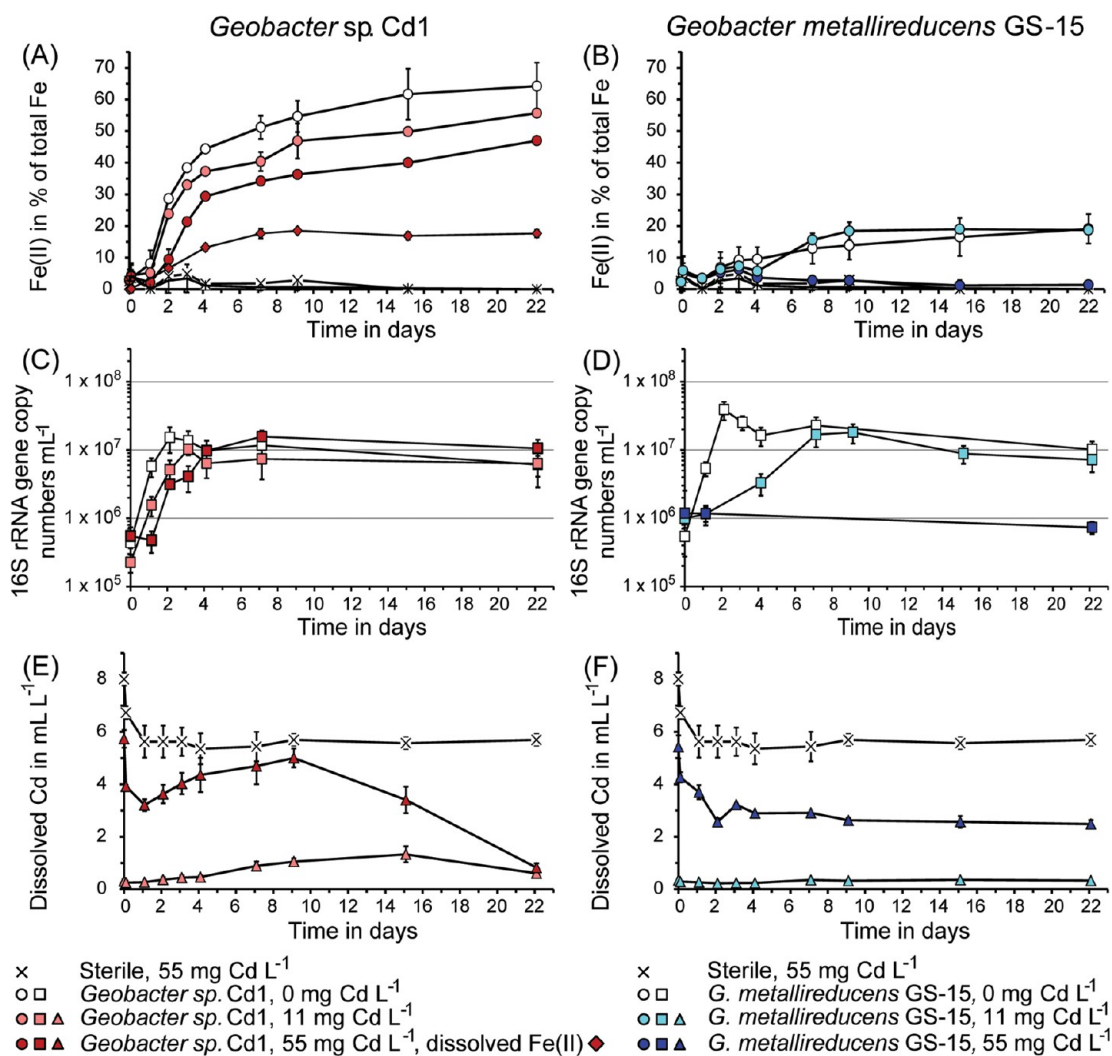


Figure 2. Fe(II) formation (A,B), 16S rRNA gene copy numbers (C,D), and concentration of mobile Cd (E,F) over time during reduction of 5 mM Cd-free and Cd-loaded ferrihydrite with 20 mM acetate by *Geobacter sp.* strain Cd1 and *Geobacter metallireducens* GS-15. Data for strain Cd1 is shown in red (A,C,E) and for strain GS-15 in blue (B,D,F). Increasing concentrations in Cd are represented by increasing color intensity. The set-ups contained either no Cd (white symbols) or 11 mg/L Cd (light red and blue) or 55 mg/L Cd (dark red and blue). Sterile controls are represented by cross symbols and data for dissolved Fe²⁺ is only shown for strain Cd1 and set-ups containing 55 mg/L Cd²⁺. Data represent the mean ± range of duplicate cultures.

HCl extractable fraction at “river” and “road”, respectively, which is considered the bioavailable Cd fraction.

Culture-dependent enumeration of Fe(III)-reducing bacteria revealed equal numbers of acetate- and lactate-oxidizing Fe(III)-reducers at each sampling site (Figure 1d), while in total, ten-times more Fe(III)-reducers were present at “river” compared to “road” (approximately 10³ and 10² cells g⁻¹ dry soil, respectively). PCR-based quantification of 16S rRNA gene copy numbers showed that in total 10⁸ bacterial 16S rRNA gene copies g⁻¹ dry soil were present at all sampling locations of the transect at Langelsheim with about 1% belonging to *Geobacter* spp. (Figure 1e).

Isolation and Phylogeny of Strain Cd1. An enrichment culture with ferrihydrite as electron acceptor and acetate as electron donor in the presence of 11 mg L⁻¹ Cd was obtained from the MPN enumeration at sampling point “river”. The enrichment was repeatedly transferred until constant Fe(III) reduction rates were obtained and one dominant cell morphology was observed microscopically. 16S rRNA sequencing and classification indicated that strain Cd1 is affiliated to the

genus *Geobacter* within the phylum *Proteobacteria*. Based on 16S rRNA gene comparison strain Cd1 has 94.6% sequence similarity to *Geobacter metallireducens* GS-15.⁴⁵ Its closest relative is *Geobacter argillaceus* strain G12 with 98.9% similarity.⁴⁶ qPCR of the Langelsheim transect revealed that strain Cd1 comprised approximately 1% of all *Geobacter* spp. at that site (Figure 1e). Cells of strain Cd1 grown in liquid cultures with acetate and fumarate appeared whitish and slightly pink. The cells were rod-shaped, 1–2 μm long and 0.3–0.4 μm wide after chemical fixation and critical point drying (Figure 1f) and were often closely associated with Fe(III) minerals in liquid cultures. When not in contact with minerals some cells showed motility. Using acetate as electron donor, strain Cd1 reduced approximately 50% of 5 mM ferrihydrite within 6 days (Figure 2). Strain Cd1 reduced ferrihydrite using a number of electron donors, namely acetate, lactate, H₂, glucose, succinate, propionate, butyrate, pyruvate, ethanol, but not formate (data not shown). Strain Cd1 was not able to grow on nitrate, nitrite or sulfate in combination with acetate and did not oxidize Fe(II) with nitrate as electron acceptor.

Microbial Fe(III) Reduction and Cd Mobility. Alongside microbial Fe(III) reduction, Cd mobility and 16S rRNA gene copy numbers were monitored for cultures of *Geobacter* sp. Cd1 and compared to *G. metallireducens* GS-15 (Figure 2). Strain Cd1 reduced Fe(III) even in the presence of 112 mg L⁻¹ Cd (data for up to 55 mg Cd L⁻¹ shown in Figure 2a), although the extent and rate of Fe(III) reduction decreased with increasing Cd concentrations. In the absence of Cd, strain Cd1 reduced 64.2 ± 7.4% of the ferrihydrite in 22 days at a maximum rate of 0.91 ± 0.05 mM Fe(II) day⁻¹, while strain GS-15 reduced 19.2 ± 4.6% Fe(III) with a maximum rate of 0.21 ± 0.10 mM Fe(II) day⁻¹ (Figure 2a,b). The presence of 11 mg Cd L⁻¹ did not significantly change the extent or rate of Fe(III) reduction for both strains, although the onset of Fe(III) reduction was delayed in GS-15 for at least one day. The addition of 55 mg Cd L⁻¹ decreased Fe(III) reduction by strain Cd1 to 47.0 ± 1.2% at a maximum rate of 0.5 ± 0.07 mM Fe(II) day⁻¹, while strain GS-15 was not able to perform Fe(III) reduction at all.

Analyzing the solid/liquid phase fractionation of Fe during ferrihydrite reduction in the presence of 55 mg Cd L⁻¹ by strain Cd1 indicated that most of the formed Fe(II) was in solution as Fe²⁺ at the beginning of Fe(III) reduction and precipitated over time with approximately 40% of the produced Fe(II) remaining in solution (Fe²⁺ data for 55 mg Cd L⁻¹ in Figure 2a).

The change in 16S rRNA gene copy numbers (as proxy for total cell numbers) over time for ferrihydrite incubations with strain Cd1 and GS-15 (Figure 2c,d) reflected the results obtained for Fe(III) reduction and increased from approximately 10⁵ cells mL⁻¹ at the start of incubation to approximately 10⁷ cells mL⁻¹ after 7 days of ferrihydrite reduction for both strains. Addition of Cd at concentrations of 11 and 55 mg L⁻¹ did not affect the final 16S rRNA gene copy numbers of strain Cd1, but progressively delayed Cd1 growth by up to 1 day, in agreement with delayed ferrihydrite reduction. In contrast to strain Cd1, *Geobacter* strain GS-15 did not grow and was unable to reduce ferrihydrite in the presence of 55 mg Cd L⁻¹. However, in the presence of 11 mg Cd L⁻¹, strain GS-15 reached the same 16S rRNA gene copy numbers after 7 days as in the absence of Cd after 2 days, thus reflecting the delay in ferrihydrite reduction observed.

Aqueous Cd concentrations in the sterile controls decreased slightly within 24 h and then remained at a constant level (Figure 2e,f). This initial drop in aqueous Cd due to equilibration of sorbed and dissolved Cd was observed for all sterile and nonsterile set-ups. For the 55 mg Cd L⁻¹ setup with Cd1, aqueous Cd concentrations increased simultaneously to the onset of ferrihydrite reduction within the first 9 days, and subsequently decreased to almost 0 by day 22. For the 55 mg Cd L⁻¹ setup of strain GS-15, dissolved Cd concentrations decreased in the first 2 days, but did not change subsequently, in agreement with the inability of this strain to sustain growth under these conditions (Figure 2f). For the 11 mg Cd L⁻¹ setup with Cd1, aqueous Cd started below 0.04 mg L⁻¹ and increased slowly to 1.3 ± 0.3 mg L⁻¹ by day 15 before it decreased again slightly (Figure 2e). By contrast, aqueous Cd in the 11 mg Cd L⁻¹ setup with strain GS-15 remained largely constant over the duration of the experiment, despite the ability of this strain to grow under this condition.

Localization of Cd in Cell-Mineral Aggregates and Mineralogy of Reduced Cd-Bearing Minerals. The distribution of Cd in the minerals before and after 31 days of ferrihydrite reduction by strain Cd1 in the presence of 55 mg

Cd L⁻¹ was followed using STXM (Figure 3). Generally, Cd was detected, but it was not found directly associated with, or

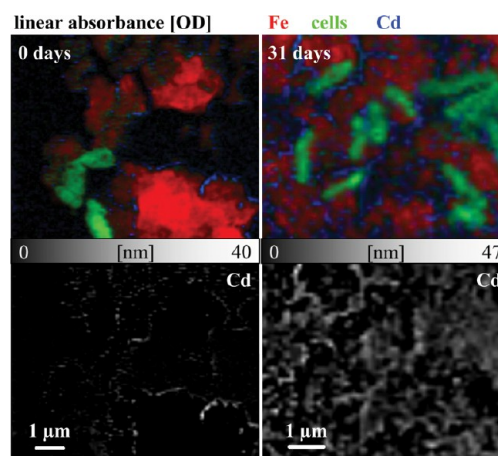


Figure 3. Scanning transmission X-ray microscopy analysis of minerals before (0 days) and after (31 days) microbial reduction of Cd-loaded ferrihydrite (8 mM ferrihydrite, 55 mg/L Cd²⁺) by *Geobacter* sp. strain Cd1. The linear absorbance of Fe (red), cells (green) and Cd (blue) in the cell-mineral aggregates are presented quantitatively as RGB values in the upper pair of panels. For better illustration of the Cd distribution within precipitates, the gray scale images of Cd alone are displayed additionally (bottom pair of panels).

within the *Geobacter* Cd1 cells. Initially, Cd was mainly associated with the surface of the ferrihydrite. After 31 days of microbial Fe(III) reduction, Cd was found to no longer be surface-associated, but rather homogeneously distributed throughout the mineral aggregates (Figure 3).

Using SEM, three different mineral morphologies were observed and analyzed by EDX to obtain Cd, Ca, P, and Fe distribution patterns. The most dominant phase was similar to the initial phase and is probably a ferrihydrite-like structure, which contained some associated Cd, Ca, and P (data not shown). The second dominant phase (Figure 4a) also contained some Cd and Ca plus a significant amount of P and Fe (Figure 5). The morphology and composition suggest the mineral vivianite [Fe₃(PO₄)₂ × 8H₂O], which was identified with Mössbauer spectroscopy (Figure 4c,d). The third mineral phase, a double-rounded aggregate made up of many needle-shaped crystallites (Figure 4b), was not present in large numbers, but contained 2–5 times more Cd than the other phases, in addition to some Fe, Ca, and almost no P (Figure 5). Based on EDX quantifications, this phase contained 1.6–1.7 times as much Ca as the other phases, however, there was approximately 3 times more Cd than Ca (atom-%). Correspondingly, a Fe-carbonate mineral was identified with Mössbauer spectroscopy (Figure 4c) suggesting that this mineral was a carbonate, potentially otavite [CdCO₃] with some Fe and Ca substituting for Cd.

Analysis of the initial, Cd-loaded minerals by synchrotron-based XRD showed two broad signals at 2-theta values of approximately 4.8° ($d = \sim 2.54$ Å) and 8.2° ($d = \sim 1.5$ Å) which are characteristic for 2-line ferrihydrite (Figure 4e). The corresponding pair distribution functions (PDF) of the XRD spectra supported the identification of the starting material as ferrihydrite (Figure 4f). After microbial Fe(III) reduction, we observed notable differences in peak intensities in the 3 and 3.5 Å region in the Cd-loaded ferrihydrite. The coherent

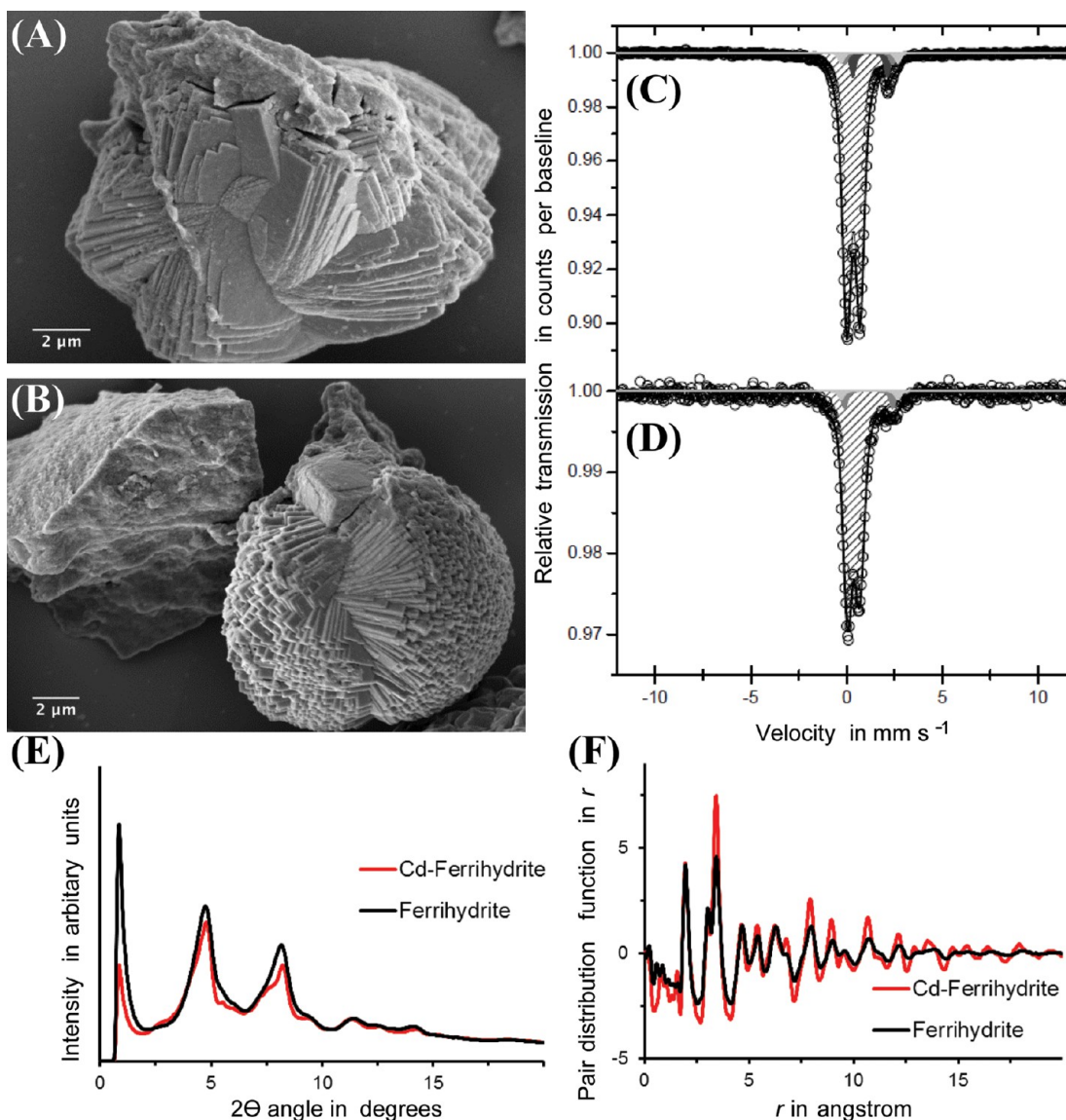


Figure 4. Characterization of the mineral products from microbial reduction of Cd-preloaded ferrihydrite (8 mM) by *Geobacter* sp. strain Cd1. Scanning electron micrographs of two mineral phases, one rich in P (A) and the other rich in Cd (B), that are present after the microbial reduction of Cd-loaded ferrihydrite. Mössbauer spectrum of the Fe mineral products in the presence of Cd (C) and absence of Cd (D) obtained at room temperature. Hatched doublet: (super)paramagnetic ferrihydrite; dark gray doublet: siderite; gray and light gray doublets: vivianite. X-ray diffractograms of Cd-loaded (red) and Cd-free (black) Fe mineral products (E) and corresponding pair distribution functions (PDF) (F).

scattering domain of the final Cd-containing mineral product extended to approximately 3 nm (Figure 4f), which is more than for pure ferrihydrite with approximately 2.2 nm. The strong increase in signal intensity above 5 Å (Figure 4f) suggests that Cd is not just surface bound but is rather a structural component of the mineral phase. Additional features in the XRD and PDF analysis point toward the presence of secondary mineral phases, including a potential phosphate-containing mineral phase based on the P–O bond observed in the 1.52 Å region (Figure 4f).

Mössbauer analysis confirmed that the starting Fe(III) minerals consisted of 2-line ferrihydrite both in the absence and presence of Cd (SI Figure S1). After 9 days of microbial reduction, unaltered ferrihydrite remained and vivianite was identified as a secondary ferrous mineral phase. After 31 days of incubation, remaining Fe(III) was identified as ferrihydrite of a higher degree of crystallinity and/or a larger particle size (SI

Figure S2). Neither magnetite, nor goethite were detected at any time during the Fe(III) reduction experiments. After 31 days of microbial Fe(III) reduction in the presence of Cd, a low-Ca, Fe-rich carbonate was identified as an additional secondary mineral product (Figure 4c).⁴⁷ This phase was absent in the Mössbauer spectra of samples after 31 days of microbial Fe(III) reduction in the absence of Cd (Figure 4d).

DISCUSSION

Fe- and Cd-Rich Field Site and Isolation of the Cd-Tolerant Fe(III)-Reducing Bacterium *Geobacter* Strain Cd-1. The field site Langelsheim is an alluvial meadow of the river Innerste near Goslar, Germany. The area is contaminated with Cd and other metals by mining and industrial activities⁴⁸ and is a natural habitat of the Cd-hyperaccumulating plant *Arabidopsis halleri*.⁴⁹ The low TIC content and pH of 6 at Langelsheim suggest that most of the Cd was mobile or

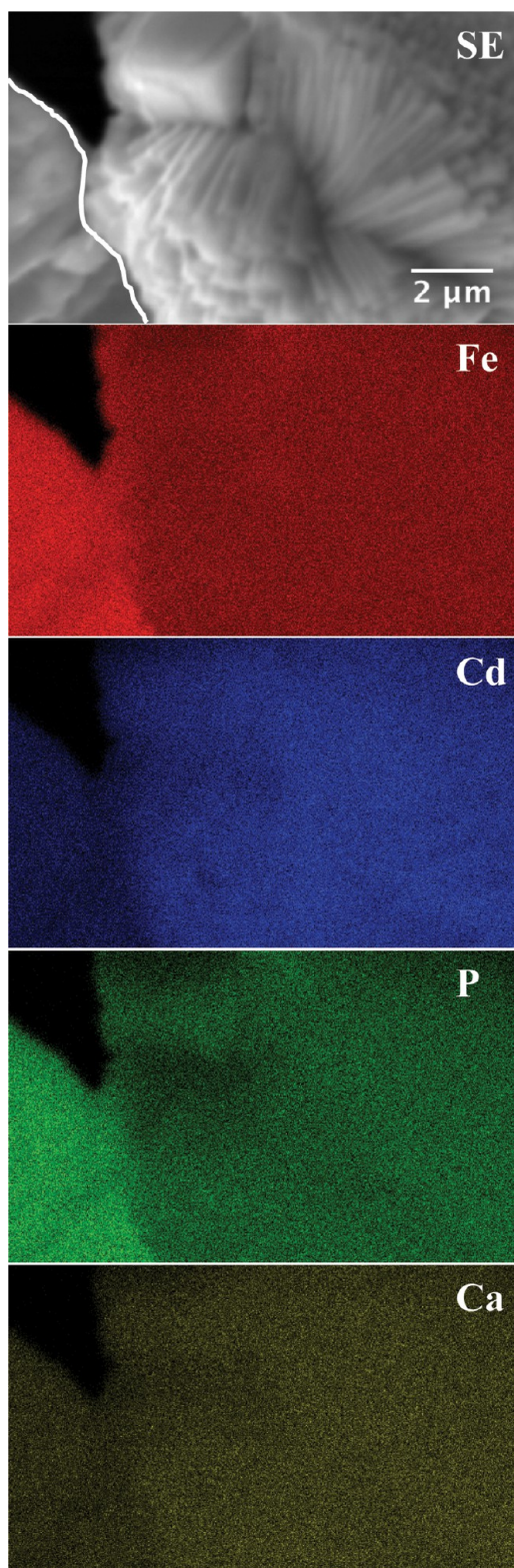


Figure 5. Energy-dispersive X-ray spectroscopy image of the Cd-rich mineral phase: Two different mineral phases can be observed, which are separated by a white line for easier identification. SE = secondary electrons. The four colored panels show distribution of Fe, Cd, P, and Ca.

associated with soil particles containing clay and ferric iron minerals⁵⁰ and not associated with carbonates. Since Langelsheim soil is rich in Fe(III), a significant fraction of Cd is

expected to be sorbed or coprecipitated with Fe(III) minerals including poorly crystalline Fe(III) (oxyhydr)oxides⁵¹ and goethite.⁵²

The organic carbon present in Langelsheim soil (4.5–8%) is a potential electron donor for microbial Fe(III) respiration,²¹ which takes place in anoxic habitats in the presence of Fe(III)-bearing minerals.⁵³ At the sampling point “road” of the field site Langelsheim, high levels of Fe(II) were indeed detected in the 0.5 and 6 M HCl extractable Fe fraction, indicating the activity of Fe(III)-reducing bacteria. The presence of organic matter might also increase the solubility of Cd by complexation or displacement from mineral surfaces via sorption competition,^{12,54} thus, increasing Cd availability to the biosphere and forcing microorganisms to adapt to the toxicity of mobile Cd.⁵⁵ Total cell numbers of 10^8 g⁻¹ dry soil at Langelsheim are in the lower range of reported cell numbers in soils,⁵⁶ indicating that the elevated metal content at Langelsheim only allowed adapted, Cd-tolerant microorganisms to thrive. Using qPCR-based quantification, we found that Fe(III)-reducing *Geobacter* spp. represent 1% of all *Bacteria* at the field site. Even though this number seems low, we have recently shown that under reducing conditions in a Cd-bearing soil, numbers of *Geobacter* spp. can increase significantly and influence the mobility of Fe and Cd.⁵⁷ Considering that other Fe(III)-reducing genera including *Shewanella* and *Desulfuromonas* coexist, the fraction of microorganisms capable of Fe(III) reduction is probably even higher than 1%.

In addition to qPCR quantification, we demonstrated in culture-dependent MPN studies the ability of bacteria from the field site to reduce Fe(III) in the presence of 11 mg Cd L⁻¹. Heavy metal tolerance has been observed before in other Fe(III)-reducing microbial communities that were dominated by *Geobacter* species, with the same maximum Cd tolerance level of 11 mg L⁻¹.⁵⁸ From our MPN enrichments, a *Geobacter* sp. strain Cd1 was isolated that performs Fe(III) reduction in the presence of 112 mg Cd L⁻¹, of which approximately 15 mg L⁻¹ were mobile, the highest Cd concentration reported so far that still allowed microbial Fe(III) reduction. In order to thrive in Cd-contaminated habitats, the microorganisms need to be adapted to metal tolerance, which can be mediated by metal efflux pumps encoded on the *czc* or *cad* operon.⁵⁹ Even though the metal efflux operon *czc* has been found in *Geobacter*, and was up-regulated during growth with Fe(III), it has not been directly linked to metal efflux, nor any other function in this genus so far.⁶⁰ However, Methé et al. postulated that metal efflux genes would be important to Fe(III)-reducers as these organisms mobilize high amounts of Fe²⁺ and other toxic metals. More support for an active metal efflux pump that can also transport Cd out of the cells of the isolated strain Cd1 comes from STXM analysis. We showed that Cd was not accumulated inside Cd1 cells, indicating that Cd was either prevented from entering the cells or was exported.⁵⁹

Mobilization and Immobilization of Cd by the Cd-tolerant *Geobacter* sp. strain Cd1 vs *Geobacter metallireducens* GS-15. To compare the isolated strain Cd1 to a non-Cd-tolerant Fe(III)-reducer regarding their ability to reduce poorly crystalline Fe(III) and to change the mobility of Cd, *G. metallireducens* strain GS-15 was chosen. This strain has environmental relevance since it was suggested to be used for bioremediation of metal-contaminated environments.^{37,61,62} So far, *G. metallireducens* has not been studied regarding Cd tolerance, and hence, its potential use as a bioremediator for Cd-contaminated sites has not been explored. However, strain

GS-15 was not able to reduce ferrihydrite in the presence of 55 mg total Cd L⁻¹ with 4–8 mg aqueous Cd L⁻¹. In conclusion, strain GS-15 does not seem suitable for the remediation of Cd-bearing soil. In contrast, strain Cd1 grew and reduced ferrihydrite in the presence of at least up to 112 mg total Cd L⁻¹ with 15 mg aqueous Cd L⁻¹. The extent and rate of Fe(III) reduction mediated by strain Cd1 was higher compared to *G. metallireducens*, in particular when considering the lower cell number present, but decreased with increasing Cd concentration. However, strain Cd1 was still able to metabolize at extremely high Cd concentrations and is relatively versatile since it uses a number of different organic cosubstrates including lactate, making it suitable for remediation of Cd-contaminated sites or the use in bioreactors used for remediation.⁶³

Cd mobility over time during Fe(III) reduction by strain Cd1 was more complex than expected. At the beginning of the incubation, Fe(III) reduction catalyzed by strain Cd1 led to Cd mobilization within the first 9 days. In a second phase, almost all dissolved Cd was removed from solution. Based on our geochemical analyses and mineral characterization and identification we hypothesize that the initial mobilization of Cd is caused by ferrihydrite dissolution, while the sequestration of Cd into solid phases is due to the formation of secondary Fe minerals. A similar behavior including mobilization and binding to secondary Fe minerals has been described before for arsenic. In Southeast Asian groundwater aquifers, arsenic is believed to be released during reductive dissolution of arsenic-bearing Fe(III) (oxyhydr)oxides.³¹ It has been demonstrated, however, that depending on the geochemical conditions, this process can also lead to the formation of secondary Fe minerals that coprecipitate/sorb arsenic.^{33,41,64}

Changes in contaminant mobility are crucial to the health and functioning of ecosystems.²⁴ In case of Cd, a sudden rise in bioavailable Cd could diminish the diversity and abundance of the microbial community significantly, while reduced mobile Cd concentrations would allow previously nontolerant microorganisms to grow—broadening the diversity and abundance of the microbial community. The observed changes in bioavailable Cd could also be useful for the remediation of Cd-contaminated sites. On the one hand, mobilized Cd could be taken up by phyto-remediating plants such as *A. halleri*, facilitating the permanent removal of Cd from contaminated sites.⁴⁹ On the other hand, the coprecipitation of Cd with secondary mineral phases would result in lower bioavailability of Cd at contaminated sites, relieving the ecosystems of a toxic stressor.²⁴

Mineral Transformation of Cd-Loaded Ferrihydrite During Fe(III) Reduction. After initial mobilization of Cd during reduction of Cd-loaded ferrihydrite, Cd was removed from solution. Approximately 47% of the Fe(III) in Cd-loaded ferrihydrite (total Cd concentration of 55 mg L⁻¹) were reduced to Fe(II) (Figure 2). The removal of Cd correlated with the precipitation of more than half of the formed Fe(II) as secondary Fe(II) minerals, while the rest of the Fe(II) remained in solution as dissolved Fe²⁺. A combination of Mössbauer and SEM-EDX analysis revealed that vivianite [Fe₃(PO₄)₂ × 8H₂O]⁶⁵ was formed as a consequence of the 1 mM phosphate present in the medium. The solubility product (25 °C) of the Fe(II)-phosphate vivianite is 10⁻³⁶ mol² L⁻², while it is 10⁻³³ mol² L⁻² for Cd-phosphate, suggesting that most of the phosphate precipitated with the Fe and not with Cd. A similar formation of Fe phosphates in the environment

has been observed in anoxic aquifers in Southeast-Asia containing fertilizer-derived phosphates.⁶⁶

Fe-specific Mössbauer spectroscopy and SEM-EDX consistently indicated carbonate mineral formation, such as otavite [CdCO₃], siderite [FeCO₃] and calcite [CaCO₃]. Note that when we talk about Mössbauer analysis of otavite or other non-Fe-containing carbonate minerals, we refer to minerals where a minor amount of the cation, that is Cd²⁺ or Ca²⁺, respectively, was substituted by Fe²⁺, thus enabling to measure Mössbauer spectra. We did not find any references for Mössbauer parameters of Fe-doped otavite in the literature. As Ca²⁺ (114 pm⁶⁷) has a very similar ionic radius to Cd²⁺ (109 pm⁶⁷) in octahedral coordination, we expect that Fe-doped otavite should have Mössbauer parameters similar to Fe-containing calcite [CaCO₃] or a high-Ca carbonate such as ankerite.⁴⁸ However, the Mössbauer parameters of the carbonate suggest the presence of a low-Ca and low-Cd carbonate such as siderite [FeCO₃] (SI Table S1). As a consequence of microbial ferrihydrite reduction, aqueous Fe²⁺ and Cd²⁺ reached their solubility maxima in the medium. Since the Cd-carbonate otavite has the lower solubility product (10⁻¹² mol² L⁻², 25 °C), it precipitates before the Fe-carbonate siderite (10⁻¹¹ mol² L⁻²). Calcite has a solubility product of 10⁻⁹ mol² L⁻² and partially coprecipitated with the forming Fe- and Cd-carbonate due to the higher Ca²⁺ concentration in comparison to Cd²⁺. Hence, the Mössbauer data suggest that otavite with some Ca²⁺ and minor Fe²⁺ precipitates first, followed by siderite with a minor amount of remaining Cd²⁺ and Ca²⁺. It has to be noted that in many environments Cd- and Fe-bearing carbonates do not necessarily precipitate during Fe(III) reduction, due to degassing of the CO₂ formed resulting in lower concentrations of carbonate. However, in permanently water-logged, carbon- and nutrient-rich environments, for example, peat bogs,⁶⁸ the formation of Fe- and Cd-carbonates and Cd-phosphates are likely. Generally, the identity of the Fe minerals formed during microbial ferrihydrite reduction depends on the geochemical conditions including the presence of phosphate, humic substances, etc.^{69–71}

Mössbauer data and the difference in the coherent scattering domain above 8 Å in the PDF analysis indicate that the ferrihydrite remaining after microbial Fe(III) reduction was more crystalline than the starting material, probably due to aging of the ferrihydrite during the experiment at 28 °C, potentially even catalyzed by Fe²⁺.⁷² It was shown previously that significant amounts of ions from solution are taken up and incorporated into Fe oxides during recrystallization.⁷³ Lin, et al.⁷⁴ showed that Cd(II) was incorporated into the product of ferrihydrite aging at high Cd(II):Fe(III) molar ratios. Since in our experiments we also used high Cd(II):Fe(III) molar ratios of up to 1:10, Cd could also have been incorporated into the aged Fe(III)-containing minerals confirming the STXM data that showed a homogeneous distribution of Cd.

Environmental Implications. Microbial Fe(III) reduction and the associated dissolution of Fe(III) minerals is known to change the mobility, and hence bioavailability of Fe oxide-bound nutrients and contaminants, which strongly impacts the functioning and health of ecosystems.²⁴ In the present study, we have shown that also the mobility of Cd is affected by microbial Fe(III) reduction. As a result of extensive agriculture and related mineral and manure fertilization, more and more soils are becoming enriched with Cd. Thus, a fundamental understanding of the processes affecting the mobility and fate of Cd in the soils, such as the combined microbial cycling of Fe

and Cd, is essential. Here, we have isolated and characterized a new Cd-tolerant Fe(III)-reducing bacterium and have used this *Geobacter* strain for identification and quantification of the complex interplay of mineral dissolution, secondary mineral formation, and Cd sequestration. However, in the environment complex microbial communities including other Fe(III)-reducing microorganisms (e.g., *Shewanella*, *Geothrix*, etc.) might influence the reduction of different Fe(III) (oxyhydr)oxides and geochemical parameters such as pH and the presence of humic substances might further affect the mobility of Cd. A better understanding of how microbial Fe cycling impacts Cd mobility is necessary for the exploration and optimization of new remediation approaches of Cd-contaminated sites.

■ ASSOCIATED CONTENT

Supporting Information

Method S1 and S2, Figure S1 and S2, Table S1. This material is available free of charge via the Internet at <http://pubs.acs.org>.

■ AUTHOR INFORMATION

Corresponding Author

*(A.K.) Phone: +49-7071-2974992; fax: +49-7071-295059; e-mail: andreas.kappler@uni-tuebingen.de.

Present Address

Biological and Environmental Sciences, School of Natural Sciences, University of Stirling, Stirling FK9 4LA, Scotland, U.K.

Notes

The authors declare no competing financial interest.

■ ACKNOWLEDGMENTS

We thank C. Herth, B. Ruediger, and K. Stoegerer for assistance in the lab, T. Lösekann-Behrens for primer design and sequence data analysis, S. Flaiz and P. Kuehn for Cd analysis, W. Kürner, H. Schulz, M. Stuhler and E. Adaktylou for SEM-support, F. Zeitvogel for providing the ImageJ plugin for visualizing the 2D-scatterplots for correlative SEM-EDX map analysis, and N. Hageman for the SEM image in Figure 1f. This work was supported by the scholarship program of the German Federal Environmental Foundation to EMM and by the Emmy-Noether program of the DFG to MO (OB 362/1-1). STXM analysis was supported by NSERC (Canada), Canada Foundation for Innovation and the Canada Research Chair program. The Advanced Light Source is supported by the Director, Office of Energy Research, Office of Basic Energy Sciences, Materials Sciences Division of the U.S. Department of Energy, under Contract No. DE-AC02-05CH11231.

■ REFERENCES

- (1) UN-EP, United Nations Environment Programm - Final review of scientific information on cadmium In 2010.
- (2) Lado, L. R.; Hengl, T.; Reuter, H. I. Heavy metals in European soils: A geostatistical analysis of the FOREGS Geochemical database. *Geoderma* **2008**, *148* (2), 189–199.
- (3) EU-JRC, European Commission-Joint Research Council. *Land Management and Natural Hazards Unit - Cadmium in European Agricultural Soils*, 2010.
- (4) REACH Registration Evaluation and Authorization of Chemicals (EU). Cadmium REACH Consortium. <http://www.reach-cadmium.eu/>

- (5) Messner, B.; Bernhard, D. Cadmium and cardiovascular diseases: Cell biology, pathophysiology, and epidemiological relevance. *Biomaterials* **2010**, *23* (5), 811–822.

- (6) Verougstraete, V.; Lison, D.; Hotz, P. Cadmium, lung and prostate cancer: A systematic review of recent epidemiological data. *J. Toxicol. Environ. Health, Part B* **2003**, *6* (3), 227–255.

- (7) Huang, S. W.; Jin, J. Y. Status of heavy metals in agricultural soils as affected by different patterns of land use. *Environ. Monit. Assess.* **2008**, *139* (1–3), 317–327.

- (8) Nicholson, F. A.; Smith, S. R.; Alloway, B. J.; Carlton-Smith, C.; Chambers, B. J. An inventory of heavy metals inputs to agricultural soils in England and Wales. *Sci. Total Environ.* **2003**, *311* (1–3), 205–219.

- (9) Atafar, Z.; Mesdaghinia, A.; Nouri, J.; Homaei, M.; Yunesian, M.; Ahmadimoghaddam, M.; Mahvi, A. H. Effect of fertilizer application on soil heavy metal concentration. *Environ. Monit. Assess.* **2010**, *160* (1–4), 83–89.

- (10) US-EPA, United States Environmental Protection Agency. *The Class V Underground Injection Control Study, Appendices E: Contaminant Persistence and Mobility Factors*, 1999.

- (11) Buekers, J.; Van Laer, L.; Amery, F.; Van Buggenhout, S.; Maes, A.; Smolders, E. Role of soil constituents in fixation of soluble Zn, Cu, Ni and Cd added to soils. *Eur. J. Soil Sci.* **2007**, *58* (6), 1514–1524.

- (12) Lee, S. Z.; Allen, H. E.; Huang, C. P.; Sparks, D. L.; Sanders, P. F.; Peijnenburg, W. J. G. M. Predicting soil-water partition coefficients for cadmium. *Environ. Sci. Technol.* **1996**, *30* (12), 3418–3424.

- (13) Tessier, A.; Rapin, F.; Carignan, R. Trace-metals in oxic lake-sediments—Possible adsorption onto iron oxyhydroxides. *Geochim. Cosmochim. Acta* **1985**, *49* (1), 183–194.

- (14) Tessier, A.; Fortin, D.; Belzile, N.; DeVitre, R. R.; Leppard, G. G. Metal sorption to diagenetic iron and manganese oxyhydroxides and associated organic matter: Narrowing the gap between field and laboratory measurements. *Geochim. Cosmochim. Acta* **1996**, *60* (3), 387–404.

- (15) Randall, S. R.; Sherman, D. M.; Ragnarsdottir, K. V.; Collins, C. R. The mechanism of cadmium surface complexation on iron oxyhydroxide minerals. *Geochim. Cosmochim. Acta* **1999**, *63* (19–20), 2971–2987.

- (16) Waseem, M.; Mustafa, S.; Naeem, A.; Koper, G. J. M.; Shah, K. H. Cd²⁺ sorption characteristics of iron coated silica. *Desalination* **2011**, *277* (1–3), 221–226.

- (17) Wang, K. J.; Xing, B. S. Adsorption and desorption of cadmium by goethite pretreated with phosphate. *Chemosphere* **2002**, *48* (7), 665–670.

- (18) Trivedi, P.; Axe, L. Modeling Cd and Zn sorption to hydrous metal oxides. *Environ. Sci. Technol.* **2000**, *34* (11), 2215–2223.

- (19) Cornell, R. M.; Schwertmann, U. *The Iron Oxides: Structure, Properties, Reactions, Occurrences and Uses*, 2nd ed.; Wiley-VCH Verlag GmbH & Co. KGaA, 2003.

- (20) Kappler, A.; Straub, K. L. Geomicrobiological cycling of iron. *Mol. Geomicrobiol.* **2005**, *59*, 85–108.

- (21) Lovley, D. R. Dissimilatory metal reduction. *Annu. Rev. Microbiol.* **1993**, *47*, 263–290.

- (22) Weber, K. A.; Achenbach, L. A.; Coates, J. D. Microorganisms pumping iron: Anaerobic microbial iron oxidation and reduction. *Nat. Rev. Microbiol.* **2006**, *4* (10), 752–764.

- (23) Shiller, A. M.; Boyle, E. A. Variability of dissolved trace-metals in the Mississippi river. *Geochim. Cosmochim. Acta* **1987**, *51* (12), 3273–3277.

- (24) Borch, T.; Kretzschmar, R.; Kappler, A.; Van Cappellen, P.; Ginder-Vogel, M.; Voegelin, A.; Campbell, K. Biogeochemical redox processes and their impact on contaminant dynamics. *Environ. Sci. Technol.* **2010**, *44* (1), 15–23.

- (25) Islam, F. S.; Gault, A. G.; Boothman, C.; Polya, D. A.; Charnock, J. M.; Chatterjee, D.; Lloyd, J. R. Role of metal-reducing bacteria in arsenic release from Bengal delta sediments. *Nature* **2004**, *430* (6995), 68–71.

- (26) Landa, E. R.; Phillips, E. J. P.; Lovley, D. R. Release of Ra-226 from uranium mill tailings by microbial Fe(III) reduction. *Appl. Geochem.* **1991**, *6* (6), 647–652.
- (27) Williams, A. G. B.; Scherer, M. M. Kinetics of Cr(VI) reduction by carbonate green rust. *Environ. Sci. Technol.* **2001**, *35* (17), 3488–3494.
- (28) Fendorf, S.; Wielinga, B. W.; Hansel, C. M. Chromium transformations in natural environments: The role of biological and abiological processes in chromium(VI) reduction. *Int. Geol. Rev.* **2000**, *42* (8), 691–701.
- (29) Holmes, D. E.; Finneran, K. T.; O'Neil, R. A.; Lovley, D. R. Enrichment of members of the family *Geobacteraceae* associated with stimulation of dissimilatory metal reduction in uranium-contaminated aquifer sediments. *Appl. Environ. Microbiol.* **2002**, *68* (5), 2300–2306.
- (30) Wielinga, B.; Bostick, B.; Hansel, C. M.; Rosenzweig, R. F.; Fendorf, S. Inhibition of bacterially promoted uranium reduction: Ferric (hydr)oxides as competitive electron acceptors. *Environ. Sci. Technol.* **2000**, *34* (11), 2190–2195.
- (31) Fendorf, S.; Michael, H. A.; van Geen, A. Spatial and temporal variations of groundwater arsenic in South and Southeast Asia. *Science* **2010**, *328* (5982), 1123–1127.
- (32) Meharg, A. A. *Venomous Earth: How Arsenic Caused the World's Worst Mass Poisoning*; Macmillan & Co, 2005; Vol. 69, p 224–225.
- (33) Kocar, B. D.; Herbel, M. J.; Tufano, K. J.; Fendorf, S. Contrasting effects of dissimilatory iron(III) and arsenic(V) reduction on arsenic retention and transport. *Environ. Sci. Technol.* **2006**, *40* (21), 6715–6721.
- (34) Hery, M.; van Dongen, B. E.; Gill, F.; Mondal, D.; Vaughan, D. J.; Pancost, R. D.; Polya, D. A.; Lloyd, J. R. Arsenic release and attenuation in low organic carbon aquifer sediments from West Bengal. *Geobiology* **2010**, *8* (2), 155–168.
- (35) Lear, G.; Song, B.; Gault, A. G.; Polya, D. A.; Lloyd, J. R. Molecular analysis of arsenate-reducing bacteria within Cambodian sediments following amendment with acetate. *Appl. Environ. Microbiol.* **2007**, *73* (4), 1041–1048.
- (36) Lee, K. Y.; Bosch, J.; Meckenstock, R. U. Use of metal-reducing bacteria for bioremediation of soil contaminated with mixed organic and inorganic pollutants. *Environ. Geochem. Health* **2012**, *34*, 135–142.
- (37) Boukhalfa, H.; Icopini, G. A.; Reilly, S. D.; Neu, M. P. Plutonium(IV) reduction by the metal-reducing bacteria *Geobacter metallireducens* GS15 and *Shewanella oneidensis* MR1. *Appl. Environ. Microbiol.* **2007**, *73* (18), 5897–5903.
- (38) Lloyd, J. R.; Lovley, D. R. Microbial detoxification of metals and radionuclides. *Curr. Opin. Biotechnol.* **2001**, *12* (3), 248–253.
- (39) Rijal, M. L.; Porsch, K.; Appel, E.; Kappler, A. Magnetic signature of hydrocarbon-contaminated soils and sediments at the former oil field Hanigsen, Germany. *Stud. Geophys. Geod.* **2012**, *56* (3), 889–908.
- (40) Kleinert, S.; Muehe, E. M.; Posth, N. R.; Dippon, U.; Daus, B.; Kappler, A. Biogenic Fe(III) minerals lower the efficiency of iron-mineral-based commercial filter systems for arsenic removal. *Environ. Sci. Technol.* **2011**, *45* (17), 7533–7541.
- (41) Muehe, E. M.; Scheer, L.; Daus, B.; Kappler, A. Fate of arsenic during microbial reduction of biogenic vs. abiogenic As-Fe(III)-mineral co-precipitates. *Environ. Sci. Technol.* **2013**, *47*, 8297–8307.
- (42) Stookey, L. L. Ferrozine—a new spectrophotometric reagent for iron. *Anal. Chem.* **1970**, *42* (7), 779–781.
- (43) Lovley, D. R.; Stolz, J. F.; Nord, G. L.; Phillips, E. J. P. Anaerobic production of magnetite by a dissimilatory iron-reducing microorganism. *Nature* **1987**, *330* (6145), 252–254.
- (44) Porsch, K.; Kappler, A. FeII oxidation by molecular O₂ during HCl extraction. *Environ. Chem.* **2011**, *8* (2), 190–197.
- (45) Lovley, D. R.; Phillips, E. J. P. Novel mode of microbial energy-metabolism—Organic-carbon oxidation coupled to dissimilatory reduction of iron or manganese. *Appl. Environ. Microbiol.* **1988**, *54* (6), 1472–1480.
- (46) Shelobolina, E. S.; Nevin, K. P.; Blakeney-Hayward, J. D.; Johnsen, C. V.; Plaia, T. W.; Krader, P.; Woodard, T.; Holmes, D. E.; VanPraagh, C. G.; Lovley, D. R. *Geobacter pickeringii* sp. nov., *Geobacter argillaceus* sp. nov. and *Pelosinus fermentans* gen. nov., sp. nov., isolated from subsurface kaolin lenses. *Int. J. Syst. Evol. Microbiol.* **2007**, *57*, 126–135.
- (47) Morris, R. V.; Ruff, S. W.; Gellert, R.; Ming, D. W.; Arvidson, R. E.; Clark, B. C.; Golden, D. C.; Siebach, K.; Klingelhofer, G.; Schroder, C.; Fleischer, L.; Yen, A. S.; Squyres, S. W. Identification of carbonate-rich outcrops on Mars by the Spirit rover. *Science* **2010**, *329* (5990), 421–424.
- (48) Knolle, F. Harzbürtige Schwermetallkontaminationen in den Flußgebieten von Oker, Innerste, Leine und Aller. *Beiträge zur Naturkunde Niedersachsens* **1989**, *42* (2), 53–60.
- (49) Kramer, U. *Metal hyperaccumulation in plants*. In *Annual Review of Plant Biology*; Merchant, S., Briggs, W. R., Ort, D., Eds.; Annual Reviews: Palo Alto, 2010; Vol. 61, pp 517–534.
- (50) Bradl, H. B. Adsorption of heavy metal ions on soils and soils constituents. *J. Colloid Interface Sci.* **2004**, *277* (1), 1–18.
- (51) Spadini, L.; Schindler, P. W.; Charlet, L.; Manceau, A.; Ragnarsdottir, K. V. Hydrous ferric oxide: Evaluation of Cd-HFO surface complexation models combining Cd-K EXAFS data, potentiometric titration results, and surface site structures identified from mineralogical knowledge. *J. Colloid Interface Sci.* **2003**, *266* (1), 1–18.
- (52) Venema, P.; Hiemstra, T.; van Riemsdijk, W. H. Multisite adsorption of cadmium on goethite. *J. Colloid Interface Sci.* **1996**, *183* (2), 515–527.
- (53) Wessel, A. K.; Hmelo, L.; Parsek, M. R.; Whiteley, M. Going local: Technologies for exploring bacterial microenvironments. *Nat. Rev. Microbiol.* **2013**, *11* (5), 337–348.
- (54) Song, Y. T.; Swedlund, P. J.; Singhal, N.; Swift, S. Cadmium(II) speciation in complex aquatic systems: A study with ferrihydrite, bacteria and an organic ligand. *Environ. Sci. Technol.* **2009**, *43* (19), 7430–7436.
- (55) Silver, S. Bacterial resistances to toxic metal ions—A review. *Gene* **1996**, *179* (1), 9–19.
- (56) Torsvik, V.; Sørheim, R.; Goksøyr, J. Total bacterial diversity in soil and sediment communities—A review. *J. Ind. Microbiol.* **1996**, *17* (3–4), 170–178.
- (57) Muehe, E. M.; Adaktylou, I. J.; Obst, M.; Zeitvogel, F.; Behrens, S.; Planer-Friedrich, B.; Kramer, U.; Kappler, A., Organic carbon and reducing conditions lead to cadmium immobilization by secondary Fe mineral formation in a pH neutral soil. *Environ. Sci. Technol.* (accepted).
- (58) Burkhardt, E. M.; Bischoff, S.; Akob, D. M.; Buchel, G.; Küsel, K. Heavy metal tolerance of Fe(III)-reducing microbial communities in contaminated creek bank soils. *Appl. Environ. Microbiol.* **2011**, *77* (9), 3132–3136.
- (59) Bruins, M. R.; Kapil, S.; Oehme, F. W. Microbial resistance to metals in the environment. *Ecotoxicol. Environ. Saf.* **2000**, *45* (3), 198–207.
- (60) Methé, B. A.; Webster, J.; Nevin, K.; Butler, J.; Lovley, D. R. DNA microarray analysis of nitrogen fixation and Fe(III) reduction in *Geobacter sulfurreducens*. *Appl. Environ. Microbiol.* **2005**, *71* (5), 2530–2538.
- (61) Anderson, R. T.; Vrionis, H. A.; Ortiz-Bernad, I.; Resch, C. T.; Long, P. E.; Dayvault, R.; Karp, K.; Marutzky, S.; Metzler, D. R.; Peacock, A.; White, D. C.; Lowe, M.; Lovley, D. R. Stimulating the in situ activity of *Geobacter* species to remove uranium from the groundwater of a uranium-contaminated aquifer. *Appl. Environ. Microbiol.* **2003**, *69* (10), 5884–5891.
- (62) Lovley, D. R.; Giovannoni, S. J.; White, D. C.; Champine, J. E.; Phillips, E. J. P.; Gorby, Y. A.; Goodwin, S. *Geobacter metallireducens* gen-nov sp-nov, a microorganism capable of coupling the complete oxidation of organic compounds to the reduction of iron and other metals. *Arch. Microbiol.* **1993**, *159* (4), 336–344.
- (63) Gavrilescu, M. Removal of heavy metals from the environment by biosorption. *Eng. Life Sci.* **2004**, *4* (3), 219–232.
- (64) Tufano, K. J.; Fendorf, S. Confounding impacts of iron reduction on arsenic retention. *Environ. Sci. Technol.* **2008**, *42* (13), 4777–4783.

(65) Mattievich, E.; Danon, J. Hydrothermal synthesis and Mössbauer studies of ferrous phosphates of the homologous series $\text{Fe}_3^{2+}(\text{PO}_4)_2(\text{H}_2\text{O})_n$. *J. Inorg. Nucl. Chem.* **1977**, *39* (4), 569–580.

(66) Zheng, Y.; Stute, M.; van Geen, A.; Gavrieli, I.; Dhar, R.; Simpson, H. J.; Schlosser, P.; Ahmed, K. M. Redox control of arsenic mobilization in Bangladesh groundwater. *Appl. Geochem.* **2004**, *19* (2), 201–214.

(67) Shannon, R. Revised effective ionic radii and systematic studies of interatomic distances in halides and chalcogenides. *Acta Crystallogr.* **1976**, *32* (5), 751–767.

(68) Gorham, E. Northern peatlands - role in the carbon-cycle and probable responses to climatic warming. *Ecol. Appl.* **1991**, *1* (2), 182–195.

(69) Borch, T.; Masue, Y.; Kukkadapu, R. K.; Fendorf, S. Phosphate imposed limitations on biological reduction and alteration of ferrihydrite. *Environ. Sci. Technol.* **2007**, *41* (1), 166–172.

(70) Zachara, J. M.; Kukkadapu, R. K.; Fredrickson, J. K.; Gorby, Y. A.; Smith, S. C. Biomineralization of poorly crystalline Fe(III) oxides by dissimilatory metal reducing bacteria (DMRB). *Geomicrobiol. J.* **2002**, *19* (2), 179–207.

(71) Amstetter, K.; Borch, T.; Kappler, A. Influence of humic acid imposed changes of ferrihydrite aggregation on microbial Fe(III) reduction. *Geochim. Cosmochim. Acta* **2012**, *85*, 326–341.

(72) Hansel, C. M.; Benner, S. G.; Fendorf, S. Competing Fe(II)-induced mineralization pathways of ferrihydrite. *Environ. Sci. Technol.* **2005**, *39* (18), 7147–7153.

(73) Handler, R. M.; Beard, B. L.; Johnson, C. M.; Rosso, K. M.; Scherer, M. M., Kinetics of atom exchange between aqueous Fe(II) and goethite. *Abstr. Pap. Am. Chem. Soc.* **2009**, 237.

(74) Lin, X. M.; Burns, R. C.; Lawrance, G. A. Effect of cadmium(II) and anion type on the ageing of ferrihydrite and its subsequent leaching under neutral and alkaline conditions. *Water, Air Soil Pollut.* **2003**, *143* (1–4), 155–177.